Research on Engineering Structures & Materials
journal homepage: http://www.jresm.org
Research Group

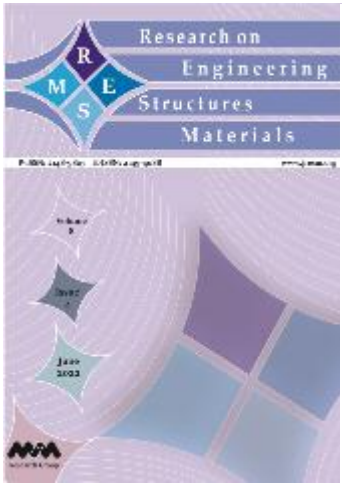

Influence of PVA and PP fibers addition on the durability and mechanical properties of engineered cementitious composites blended with silica fume and zeolite

H. Emamjomeh, K. Behfarnia, A. Raji, M. Almohammad-albakkar

Online Publication Date: 30 Dec 2022
URL: http://www.jresm.org/archive/resm2022.491me0804.html
DOI: http://dx.doi.org/10.17515/resm2022.491me0804
Journal Abbreviation: *Res. Eng. Struct. Mater.*

To cite this article
Emamjomeh H, Behfarnia K, Raji A, Almohammad-albakkar M. Influence of PVA and PP fibers addition on the durability and mechanical properties of engineered cementitious composites blended with silica fume and zeolite. *Res. Eng. Struct. Mater*., 2023; 9(2): 457-473.

Research on Engineering Structures & Materials
journal homepage: http://www.jresm.org
Research Group

Research Article

Influence of PVA and PP fibers addition on the durability and mechanical properties of engineered cementitious composites blended with silica fume and zeolite

H. Emamjomeh[a], K. Behfarnia[b], A. Raji[c], M. Almohammad-albakkar[*,d]

Department of Civil Engineering, Isfahan University of Technology, Isfahan 84156-83111, Iran

Article Info

Article history:

Received 04 Aug 2022
Revised 12 Dec 2022
Accepted 23 Dec 2022

Keywords:

ECC;
Zeolite and Silica fume;
Blast furnace slag;
Polyvinyl alcohol fibers;
Polypropylene fibers;
Magnesium sulfate environment

Abstract

Over the past two decades the effects of different admixtures have been investigated on mechanical properties and durability of engineered cementitious composites (ECC). Despite this, materials such as silica fume and zeolite have not been thoroughly investigated. The present study was designed and implemented to evaluate the effects of silica fume, zeolite, and blast furnace slag (BFS) on engineered cementitious composites and to compare the mechanical properties and durability of the polyvinyl alcohol-ECC (PVA-ECC) and polypropylene-ECC (PP-ECC) specimens. For this purpose, specimens were subjected to adverse conditions in a 5% magnesium sulfate solution and lab conditions as the reference treatment to measure the post-treatment variations in their compressive strength, flexural strength, and mid-span deflection (MSD). Results demonstrated that PP-ECC was not only easier to manufacture but outperformed PVA-ECC in some respects as well. It was also observed that MSD increased in the PVA-ECC specimens but declined in the PP-ECC ones under identical increments in their BFS contents. Finally, all the specimens maintained under the lab conditions displayed the best performance in terms of strength and durability when 3% silica fume was added to their mixtures while the same addition led to the worst performance in the sulfate medium.

1. Introduction

Although concrete has a history of more than a century in the construction industry, its durability has only recently been investigated. Degradation of concrete structures under such harmful conditions as sulfate, acidic, or chloride ion attacks, as typically occurs in coastal areas, has motivated a lot of research aimed at improving the durability of cement-based materials. Concrete deterioration in coastal areas often takes long years due to the low concentrations of aggressive ions in seawater. Most hydraulic structures are designed for a service life of 50 to 100 years depending on the intended use. Poor durability of cement-based materials, however, causes such structures to deteriorate long before their planned service life is reached [1] . This is especially true for structures in coastal areas or in aquatic environments where aggressive agents continually damaging structures are varied. The Gutianxi II Hydropower Station in China is a clear example of accelerated concrete deterioration only after 30 years of operation that incurred more than four million dollars of payouts on structural repairs [2] .

One of the adverse environmental conditions most influencing the durability of concrete hydraulic structures is sulfate attack [3]. The chemical reactions between cement hydration products and sulfate ions produce expansive chemical compounds that cause

*Corresponding author: m.almohammadalbakkar@cv.iut.ac.ir
[a] orcid.org/0000-0003-3962-7559; [b] orcid.org/0000-0003-0881-9849; [c] orcid.org/0000-0002-3372-8239; [d] orcid.org/0000-0003-1684-3080
DOI: http://dx.doi.org/10.17515/resm2022.491me0804

cracks in concrete that, in turn, allow sulfate ions or water to infiltrate into the inner parts of the structure, thereby accelerating the deterioration process [4] .

A wide variety of causes have been cited for concrete cracking under field conditions. These include mechanical loading, thermal shocks, shrinkage, unequal foundation settlement, and chemical attacks [5] , with sulfate attack being the most common cause of cracks developing within the cement-based materials that ultimately give rise to the poor durability of concrete in hydraulic structures [6, 7]. Even though cracks accelerate concrete deterioration by allowing easier penetration of aggressive ions [8-11], the impacts of cracks on the deterioration process may be trivial when they within a relatively small width range. When crack widths exceed 100 μm, however, corrosion rate grows to a large extent [12, 13]. Wang et al. reported that concrete permeability gradually increased from an uncracked state to that of crack widths 50 μm in size, beyond which a sharp increase was observed in permeability with rising crack widths from 50 to 200 μm [14]. Study has shown that, from the viewpoint of concrete durability, a crack width below 200 μm (and ideally, one below 50 μm) is desirable for hydraulic concrete structures because concrete permeability scales with the 3rd power of crack widths above 50 μm [8, 15-17]. Using electrochemical impedance spectroscopy as a non-destructive test, Zhu et al. [18] investigated the differences between engineered cementitious composites (ECC) and plain mortar in their cracking behavior. Given the fact that cracking in cement-based materials almost inevitably occurs under mechanical loading or adverse environmental conditions, it will be essential in such applications to use construction materials such as engineered cementitious composites (ECC) with potentially low crack widths. This is while ECCs offer the additional advantages of high toughness, spalling resistance, and low permeability [19-26]. Oil-coated polyvinyl alcohol (PVA) fibers have been most commonly used in the manufacture of ECC; however, recent studies show that highly ductile ECCs could also be developed using the non-oil-coated, low tensile strength PVA fiber by re-tailoring the matrix [27]. In a more recent study by Arulanandam et al. [28], an approach using a thorough analytical and finite element analysis (FE) has been used to study the performance of engineered cementitious composite (ECC) beams with and without transverse reinforcements. In a follow-up study by Maheswaran et al. [29], the shear behavior of engineered cementitious composite beams with a hybrid mix of polyvinyl alcohol (PVA) and polypropylene (PP) fibers was investigated experimentally and numerically. The primary objective of their study is to understand how ECC beams with mono and hybrid fiber combinations behave in shear under different shear scenarios. Based on the results, hybrid PVA-PP fibers were found to enhance the performance of ECC beams by improving their performance in terms of strength and ductility in comparison with steel and PP-fibers. moreover, a failure transition from brittle diagonal tension to ductile bending was observed when hybrid fibers were incorporated into ECC beams [29]. Additionally, ABAQUS software was utilized to conduct a detailed nonlinear finite element analysis [29].

Although the mechanical properties and durability of ECCs under different conditions have been investigated in recent years [30-33], only few studies, have been conducted to determine the effects of silica fume, zeolite, blast furnace slag (BFS), and different fiber types on the mechanical and durability properties of ECC. In order to fill this gap, this study examines the effects of silica fume and zeolite on ECCs in 5% magnesium sulfate solution, which is considered the most destructive environment for cement-based materials. In this context, zeolite and silica fume were selected and added to ECCs since they can improve the microstructure of the evaluated concrete; thereby enhancing its performance and permeability properties. In addition, to determine the difference between the performance of the (polyvinyl alcohol) PVA-ECC specimens subjected to the sulfate medium and lab conditions and those of the (polypropylene) PP-ECC specimens, compressive strength,

flexural strength, and midspan deflection were measured at four (28, 150, 180, and 210 days) concrete ages.

2. Experimental Program

2.1. Materials and Mix Designs

To make the ECC mixtures required in this study, type II Portland cement, silica fume, zeolite, blast furnace slag (BFS), and limestone powder (LSP) are used. In parallel, high-range water-reducing admixtures (HRWRA), polyvinyl alcohol (PVA) fibers, or polypropylene (PP) fibers were added. In addition to their great pozzolanic activity, the pozzolans used are cheap and abundant in Iran. The chemical compositions and physical properties of the powder materials are reported in Table 1 and Table 2, respectively.

Table 1. Chemical composition of the materials used (%)

Material	SiO_2	Al_2O_3	Fe_2O_3	CaO	MgO	SO_3	Na_2O	K_2O	$CaCO_3$
Cement	22.00	5.00	3.82	64.00	1.90	1.50	0.25	0.49	-
Zeolite	63.30	11.70	0.32	3.60	1.20	0.09	-	-	-
Silica fume	92.50	0.90	0.80	1.00	1.60	-	0.40	0.35	-
LSP	0.23	0.08	0.09	55.31	0.21	-	-	-	98.72
BFS	34.70	10.93	-	38.37	10.30	2.53	0.60	0.60	-

Table 2. Physical properties of the materials used

Material	Specific gravity (gr/cm^3)	Av. size (μm)	Specific surface area (m^2/kg)	L.O. I[1]
Cement	3.15	16.20	300	1.00
Zeolite	2.20	16.84	320	8.49
Silica fume	2.00	0.23	22500	1.70
LSP	2.71	13.40	460	43.43
BFS	2.80	10.60	400	0.56

[1]Loss On Ignition

Clearly, no aggregate was used in the mixtures in order to reduce the fracture toughness of the matrix formed because the presence of aggregates would increase the tortuosity of the fracture path in the ECC.

While both the fibers used were 12 mm in length, the PVA fiber measured significantly higher values of tensile strength and elasticity modulus than did the PP one. The most important difference between the fibers with regards to the properties of the ECCs produced, however, is their surface properties that make them either hydrophobic or hydrophilic. To make the PVA fibers less hydrophilic, a solution containing anti-static materials was sprayed on the fibers. Table 3 reports the mechanical properties of the fibers used in this research. A total number of 280 cube specimens, 70 mm on each side, and 280 prism ones, 350 mm × 100 mm × 30 mm in size, were cast using eight different mix designs.

Table 3. Properties of the fibers used

Fiber	Modulus of elasticity (GPa)	Tensile strength (MPa)	Tensile strain (%)	Specific gravity (gr/cm^3)	Length (mm)	Diameter (μm)
PVA	35	1588	6	1.3	12	15
PP	4.1	400	8-10	0.91	12	19

Table 4 reports the mix design proportions. The letters L, S, Z, and M in the designations used for the mix designs represent LSP, BFS, zeolite, and silica fume, respectively. The digits following each letter represent the percentage of the admixture represented relative to the whole cementitious materials used in the specimen; for example, the mixture L30 S40 M3-PVA contained 30% LSP, 40% BFS, and 3% silica fume with the remaining content being Type II Portland cement. Finally, PVA indicates that the specimen was reinforced with PVA fibers.

Table 4. ECC mix design proportions (kg/m^3)

Mix ID	Cement	BFS	LSP	Zeolite	SF	Water	HRWRA	PVA	PP
L30 S43-PVA	400	637	445	0	0	474	8	25	0
L30 S47 Z3-PVA	294	691	441	44	0	470	11	25	0
L30 S40 Z3-PVA	399	590	443	44	0	472	11	25	0
L30 S40 M3-PVA	400	593	445	0	44	474	8	25	0
L30 S43-PP	400	637	445	0	0	474	7	0	17
L30 S47 Z3-PP	294	691	441	44	0	470	8	0	17
L30 S40 Z3-PP	399	590	443	44	0	472	8	0	17
L30 S40 M3-PP	400	593	445	0	44	474	5	0	17

The parameters studied included the strength, ductility, and durability of the specimens in a medium of 5% magnesium sulfate solution. Previous study had indicated that the 5% magnesium sulfate solution was more destructive to concrete than such other sulfate solutions as sodium sulfate, particularly with respect to their effects on reducing compressive strength [34-39] . The higher values of high-range water-reducing admixture (HRWRA) reported in Table 4 for the mixtures containing zeolite are due to the porous and platy microstructure of natural zeolite.

2.2. Mixing

The materials used, mixing ratios, mixing method, ECC casting method, and its curing method are the factors with strong effects on ECC performance, especially its ductility. It may, however, be confidently maintained that the mixing method employed is the one with the greatest effect on ECC ductility. For example, in the absence of a proper mixing method, fiber balling will occur in ECC specimens with no subsequent multiple cracking and strain hardening even if all the other factors, including the materials used and their mix proportions, are ideal. Improper mixing has, indeed, a greater negative effect on ECC ductility than it does on other mechanical properties such as compressive strength. Overall, preparing good ECC specimens strongly relies on such important factors as mixing sequence, duration of each mixing step, mixer speed, mortar viscosity during fiber addition, and the rate at which fibers are added into the mixture. In the present

experiment, the following sequence was adopted for mixing the ingredients of the ECC specimens:

- Initially, all the powder constituents including cement, slag, lime powder, and silica fume or zeolite were mixed for 1 minute at 70 rpm.
- Two-thirds to three-quarters (depending on the mix design) of the water and HRWRA were added to the cementitious materials and mixed initially at 140 rpm for 2 minutes followed by mixing at 300 rpm for 1 minute.
- All the fibers were gradually added into the mixture over a period of 10 minutes while being mixed at 140 rpm. At appropriate intervals, the remaining (one-third or one-quarter) water was added to the mixture in 3 to 5 steps (depending on the mix design) and the mixer speed at each step was raised to 300 rpm for 30 seconds.
- Finally, the mixture thus obtained was mixed at 300 rpm for 3 minutes.

2.3. Testing

The ECC specimens were removed out of their molds after 48 hours to be cured in water for 26 days. Five cubes and five prisms from each mix design were subsequently tested and their compression strength and toughness were measured while half of the remaining specimens were transferred into the 5% magnesium sulfate solution and the rest were stored under lab conditions (50±5 relative humidity, 23±2° C). To avoid changes in solution concentration through time due to sulfate precipitation, the sulfate solution was regularly mixed using a timer that would turn on the water pump for 20 min per hour. In addition, all the specimens in the solution were kept adequately spaced from each other using plastic shields.

In order to compare the durability performance of different ECC mixtures treated in the magnesium sulfate solution, the variation in compressive strength, flexural strength, and MSD (MSD corresponding to maximum flexural strength) were calculated at concrete ages of 150, 180, and 210 days. In this study, all the reported results of each parameter were the averages of five measurements and compared with the control mixtures, which were also made with the same constituents and treated under lab conditions.

3. Results and Discussion

3.1. Compressive Strength

Using 70-mm cubic specimens, the compressive strengths of each mix design were measured at the ages of 28, 150, 180, 210 days. Fig. 1and Fig. 2 depict the high ability of the ECC specimens to withstand compressive strains and their cracking patterns, respectively, after the compressive test. Fig. 3 shows the compressive strengths of ECC specimens of different ages treated under lab conditions while Fig.4 presents the reductions in the compressive strength of specimens cured in the sulfate medium. In Fig.4 similar mix designs (those containing the same cementitious constituent but reinforced with different fibers) are shown by similar patterns next to each other but differentiated by different colors (the lighter color represents PP-ECC).

Fig. 1 ECC high ability to withstand compression

Fig. 2 Cracking pattern in ECC specimens due to compressive test

According to Fig. 3**,** at all the concrete ages tested, the mixtures reinforced with PP fibers recorded higher compressive strengths than those measured in the corresponding ones but reinforced with PVA fibers. The differences could have been due to the presence of the anti-static solution on PVA fibers that formed small air bubbles when mixed with water.

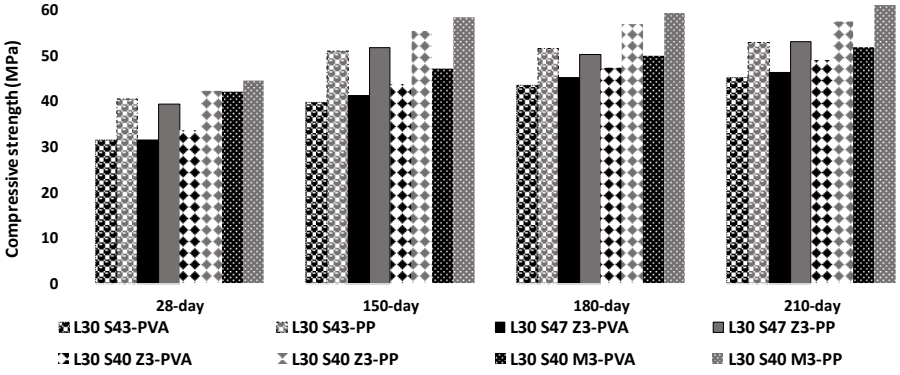

Fig. 3 Compressive strengths of the specimens of different ages treated under lab condition

This is while higher compressive strengths were recorded at all concrete ages and regardless of the fiber type used for the mixture containing silica fume (L30 S40 M3) than those recorded for the mixture containing the same amount of zeolite (L30 S40 Z3), probably due to the higher pozzolanic activity of silica fume than that of zeolite. It must be

noted that an increase of 18% in BFS used in L30 S47 Z3, compared with L30 S40 Z3, reduced its compressive strengths at all ages regardless of the fiber type used; again, this might have been due to the weaker pozzolanic activity of BFS compared to other mixture constituents.

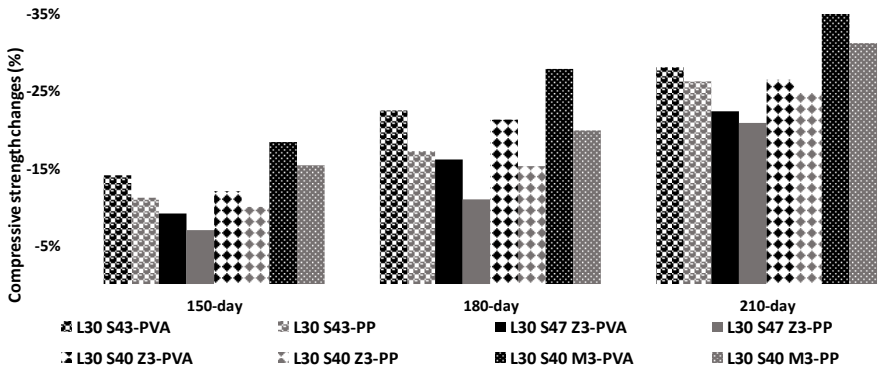

Fig. 4 Variations in the compressive strength of specimens cured in the 5% magnesium sulfate solution relative to the values measured for the control mixes

According to Fig.4, however, the increase in BFS in the specimens treated in the sulfate medium led to their better performance at all concrete ages, indicating the efficacy of BFS in maintaining ECC compressive strength when exposed to the 5% magnesium sulfate solution. This is principally attributed not only to the reduced calcium hydroxide present in the cement paste due to reaction with BFS but also to the pore structure and pore size distribution of the cement paste that were modified by BFS. Moreover, a reduction of 26.5% was observed in the compressive strength of the L30 S40 Z3-PVA specimens at the age of 210 days while the same parameter showed reductions of 24.9% in L30 S40 Z3-PP which indicate compressive strength values by 6% higher in the PP-ECC specimens subjected to a sulfate attack relative to those recorded for the PVA-ECC ones.

It may be figured out from Fig. 4 that the greatest reduction in compressive strength observed for all the three concrete ages due to treatment in the sulfate medium belonged to mixtures containing silica fume, indicating the outperformance of zeolite over silica fume in maintaining the durability of specimens treated in the magnesium sulfate solution. This is probably due to the deterioration of the cement paste as a result of C-S-H conversion into magnesium silicate hydrate (M-S-H) in mixtures containing silica fume. The better performance of the mixtures containing zeolite in sulphate medium undergoes its pozzolanic activity due to its high quantity of reactive SIO2 and Al2O3, which combines with Ca (OH)2 to form additional C-S-H gel. Comparison of L30 S43 and L30 S40 Z3 reveals that 3% zeolite used as a substitute for BFS led to a considerable improvement in the compressive strength of the specimens treated in the sulfate medium, mainly due to the limited formation of ettringite in the presence of zeolite.

A reduction of 22.4% in the compressive strength was recorded for the 210-day L30 S47 Z3-PVA specimen subjected to the sulfate attack while the same measurement for L30 S40 Z3-PVA showed 18.9% reduction. These values indicate that an 18% increment in BFS (L30 S47 Z3 vs L30 S40 Z3) was able to enhance ECC durability in a sulfate environment as a result of enhancements of 15.4% in compressive strength.

3.2. Flexural Strength

The flexural strengths of each mix design at concrete ages of 28, 150, 180, 210 days were measured using 350 x 100 x 30 mm prism specimens. Both PVA-ECC and PP-ECC showed multiple cracking patterns and strain hardening behaviors during the bending test. Fig.5 and Fig.6 illustrate the fiber bridging action and the bending test setup, respectively.

Fig. 5 Fiber bridging in the 28-day L30 S40 Z3-PP specimen at rupture

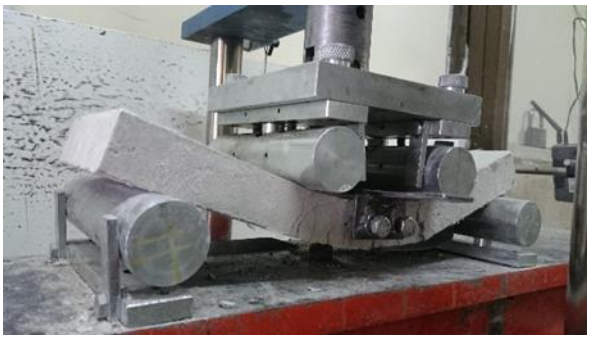

Fig. 6 Bending test of the 28-day L30 S40 Z3-PP specimen

The ECC specimens exhibited a far more complicated behavior under the bending test, especially with regard to deflection, than they did under the compressive test. This is because the compressive strength of cement composites such as ECC containing polymeric fibers is mainly influenced by the characteristics of the mortar used. In fact, neither the distribution of fibers nor the fiber-matrix bonding has any significant effect on the compressive strength of ECCs. These parameters, however, have great impacts on ECC's flexural behavior so that the study of fiber reinforced concrete behavior under bending or tension requires the impact of a combination of factors to be considered simultaneously. Put simply, any material added to the ECC mixture might lead to changes in the characteristics of the matrix, fiber-matrix interface, and fiber distribution.

Fig. 7 shows the flexural strengths of the specimens treated under lab conditions. Clearly, the mixtures reinforced with PVA fivers exhibited higher flexural strengths at all concrete ages than did the corresponding ones reinforced with PP fibers. This is due to the higher mechanical properties, particularly the higher tensile strength of PVA fibers than that of PP ones, and the higher PVA-matrix bond strength compared to that of the PP-matrix interface. The lower bond strength of the PP-matrix is due to the frictional bonding, rather than a chemical one, at this interface [40] . This is while both chemical and frictional bonds are at work at the interface of the PVA fibers with the matrix.

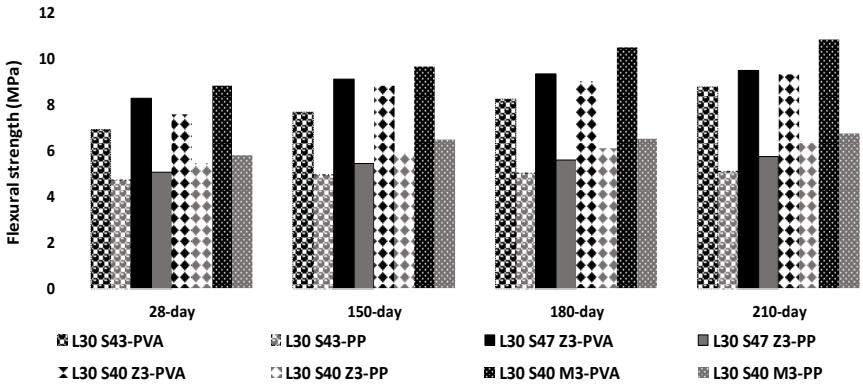

Fig. 7 Flexural strengths at different ages of specimens treated under lab conditions

The specimens with mix designs containing silica fume recorded the highest flexural strengths regardless of their fiber type or concrete age; this was attributed to the higher pozzolanic activity of silica fume compared to those of zeolite and BFS. Moreover, specimens containing silica fume and either type of fiber exhibited flexural strengths higher than did those made of other mixtures (Fig.7); this was also ascribed to the higher pozzolanic activity of silica fume that gave rise to stronger bonds at the fiber-matrix interface. In addition to its higher pozzolanic activity, silica fume leads to a more uniform distribution and, thereby, a more efficient use of fibers. The high flexural strength of mixtures containing silica fume is more pronounced when they are reinforced with PVA fibers because silica fume enhances only the frictional bonds at the PP-matrix interface but it increases both the chemical and frictional bonds at the PVA-matrix one.

An 18% increment in the BFS content of L30 S47 Z3 relative to that of L30 S40 Z3 led to an enhancement in the flexural strength of the specimens with PVA fibers but a slight decrease in that of specimens with PP fibers (Fig.7). This might be related to the effects of increased BFS content on the fiber-matrix interface that vary with the type of fibers used. More specifically, BFS increases in the studied range were observed to reduce the chemical bond strength at the PVA-matrix interface but they improved fiber distribution, the overall result of which was an increment in the specimen's flexural strength. In the case of PP fibers, however, increased BFS content, in contrast to zeolite or cement, reduced the frictional bond strength at the fiber-matrix interface although it improved fiber distribution. As a result, PP fiber slippage was observed to happen because of the poor chemical bond and the reduced frictional bond at their interface with the matrix.

Comparison of L30 S43 and L30 S40 Z3 differing only in their zeolite contents reveals that zeolite increases in the studied range enhanced flexural strength in specimens containing either fiber type and at all concrete ages (Fig.7), indicating that zeolite not only improved fiber distribution but enhanced the chemical bond as well; hence, the observed increase in flexural strength. Moreover, zeolite was observed to have a more pronounced effect on increasing flexural strength in specimens reinforced with PVA fibers while it had almost no such effect on the chemical bonds of PP fibers.

Fig.8 compares the variations in flexural strength in the specimens exposed to the sulfate medium with those of the control mixes. Clearly, the specimens reinforced with PP fibers, regardless of the mix design used or the concrete age, exhibited less reductions in their flexural strengths than did the corresponding ones reinforced with PVA fibers. For

instance, a reduction of 30% was observed in the flexural strength measurements, of the L30 S40 Z3-PVA specimens at the age of 210 days while the same parameters showed reductions of 25.4%, in L30 S40 Z3-PP which indicate flexural strength values by 15.3% higher in the PP-ECC specimens subjected to a sulfate attack relative to those recorded for the PVA-ECC ones. This is probably due to the higher quality and homogeneity of the PP-ECC specimens, due to their denser materials induced by lack of interfacial chemical bonds, than the PVA-ECC ones. A reduction of 26.1% flexural strength was recorded for the 210-day L30 S47 Z3-PVA specimen subjected to the sulfate attack while the same measurement for L30 S40 Z3-PVA showed 22.7% reduction. These values indicate that an 18% increment in BFS (L30 S47 Z3 vs L30 S40 Z3) was able to enhance ECC durability in a sulfate environment as a result of enhancements of 13% flexural strength.

Similar to the changes observed in compressive strength, higher reductions were observed in the flexural strength of the specimens containing silica fume (Fig.8), probably because of the deterioration of the cement paste by C-S-H conversion into magnesium silicate hydrate (M-S-H). These observations bear witness to the superior performance of zeolite with respect to concrete strength over silica when the specimen is under a sulfate attack.

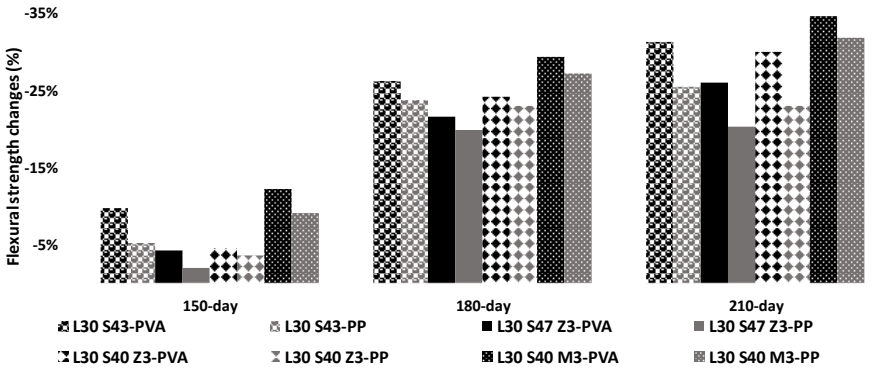

Fig. 8 Variations in flexural strength in specimens cured in the 5% magnesium sulfate solution compared with the control ones

Fig.8 also indicates that, compared to mixtures containing zeolite (namely, L30 S43 and L30 S40 Z3), those lacking in zeolite exhibited a lower resistance against the sulfate environment in terms of flexural strength. this may be explained by the pozzolanic activity of zeolite that consumes it to make a denser matrix, thereby limiting the formation of ettringite.

3.3. Midspan Deflection

Fig.9 shows the MSD values obtained for the specimens treated under lab conditions at different concrete ages. A glance at Fig.9 reveals the significantly higher MSD values of the PP-ECC specimens at all concrete ages than those of the PVA-ECC ones. This is because the lack of chemical bonds at the PP-matrix interface causes the fibers bridging across crack edges to slip due to their insufficient elongation. In contrast, the slippage distance of the PVA fibers is limited because of the presence of both the chemical and frictional bonds at the fiber-matrix interface; this might have been the main reason underlying the higher MSD values of the PP-ECC specimens. It must be reminded that the slippage of PP fibers was clearly observed during the bending test as shown in Fig.5.

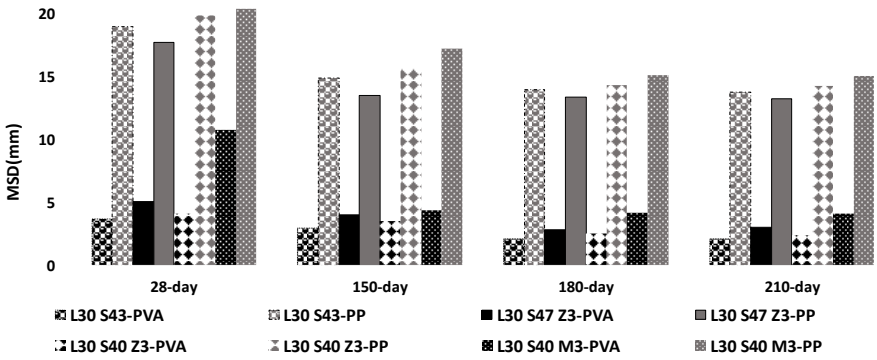

Fig. 9 MSD values at different concrete ages measured in specimens treated under lab conditions

Another interesting point observed during the bending test was the differences in crack formation on the tension side between PP-ECC and PVA-ECC specimens (Fig.10). The crack widths in the PVA-ECC specimens are clearly too small to be seen in the absence of sufficient light or with the naked eye. In contrast, crack widths in the PP-ECC specimens are larger and can be easily seen. This could be due to the higher slippage distance of the PP fibers.

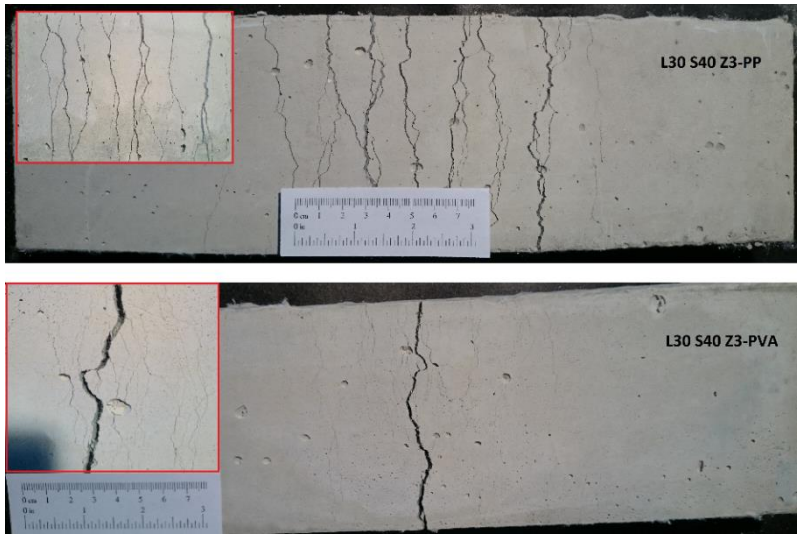

Fig. 10 Crack formation in PP-ECC *vs.* PVA-ECC specimens

The highest MSDs at all concrete ages in both PP-ECC and PVA-ECC specimens were observed in specimens with mixtures containing silica fume, which is probably because of the optimized distribution of fibers and the bond strength at the fiber-matrix interface modified due to the presence of 3% silica fume (Fig.9). Moreover, the increased BFS content gave rise to a 20.4% increment in MSD in PVA-ECC but to a 7.5% decrease in PP-ECC (L30 S47 Z3 vs. L30 S40 Z3), this could be related to the different effects of BFS content on fiber-matrix interfacial bond of PVA-ECC and PP-ECC.

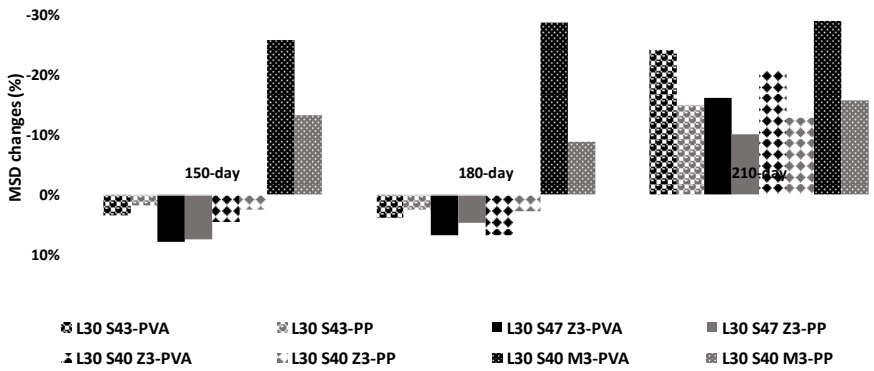

Fig. 11 Variations in MSD values recorded for specimens exposed to the 5% magnesium sulfate solution compared to those of the control ones

According to Fig. 11, MSD values increased in certain specimens while they decreased in others after treatment in the magnesium sulfate solution. This difference might have arisen from the different effects of magnesium sulfate on matrix toughness and interface bond strength in the different mixtures. One reason that can be claimed for the reduced MSD values in some mixtures is the excessive reduction in their frictional bond strength at the fiber-matrix interface below the permissible range that would allow strain-hardening to occur. On the other hand, the increased MSD values after treatment in the magnesium sulfate solution suggests that both the matrix fracture toughness and the fiber-matrix interface were modified in accordance with the strain-hardening criteria within the micromechanics theory (i.e., due to excessively reduced frictional and chemical bond strengths).

According to Fig. 11, the highest reduction in MSD values both groups of PP-ECC and PVA-ECC specimens were recorded for mixtures containing silica fume, indicating once again that silica fume is not a suitable pozzolan to fight against the adverse effects of the magnesium sulfate solution that is probably due to the conversion of C-S-H to magnesium silicate hydrate (M-S-H) that destroys cement paste, and consequently, causes higher degradation and reduces compressive strength (36). A reduction of 20.8% was observed in the MSD measurements of the L30 S40 Z3-PVA specimens at the age of 210 days while the same parameters showed reduction of 10.8% in L30 S40 Z3-PP which indicate MSD values by 48% higher in the PP-ECC specimens subjected to a sulfate attack relative to those recorded for the PVA-ECC ones.

3.4. Stress-Midspan Deflection Curve

Fig. 12 presents the stress-MSD diagrams for the 28-day PVA-ECC and PP-ECC specimens. Clearly, they all indicate an almost linear pre-cracking behavior for all the mixtures tested in addition to a strain-hardening behavior exhibited by both PVA-ECC and PP-ECC specimens. It is also seen that although the PVA-ECC mixtures obviously exhibit higher flexural strengths, their MSD values are correspondingly lower. It is also interesting to note that, compared to the PP-ECC specimens, the PVA-ECC ones exhibit steeper post-cracking slopes. The difference might be attributed to the high abrasion during the pullout stage resulting from the greater increase in the frictional bond strength at the interface in the PVA-ECC specimens than that in the PP-ECC ones.

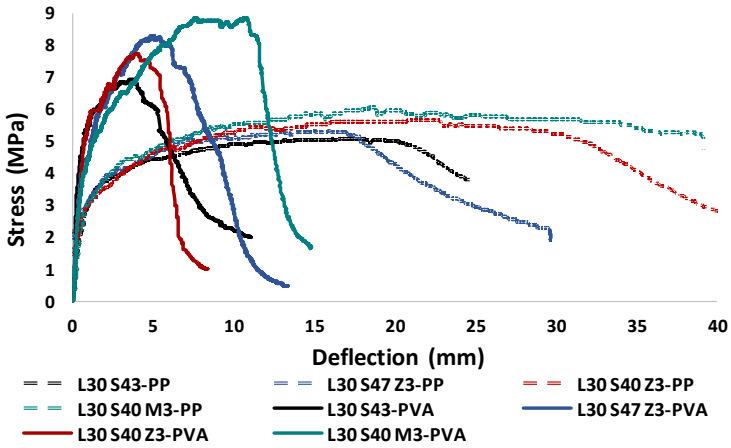

Fig. 12 PVA-ECC stress-MSD diagram

Finally, the PP-ECC specimens do not abruptly rupture after reaching their peak flexural capacity; they, rather, sustain their load-carrying capacity in a milder fashion (i.e., the negative slope in the diagram). This might be explained with recourse to the lower damage incurred by abrasion on the surface of PP fibers than on that of PVA ones.

3.5. Analysis of SEM Images

Based on Fig. 13, the SEM images of a unique mixture (L30 S43) reinforced with different fibers indicate more material bonded to PVA fibers than to PP ones. In addition, the PVA fibers endure severe damages seen as a deep longitudinal crack along the fiber. This could be due to the existence of the high chemical bonds at the PVA-matrix interface, which causes severe damages during the pullout stage. This is while the PP fibers only exhibit a slight abrasion on the surface.

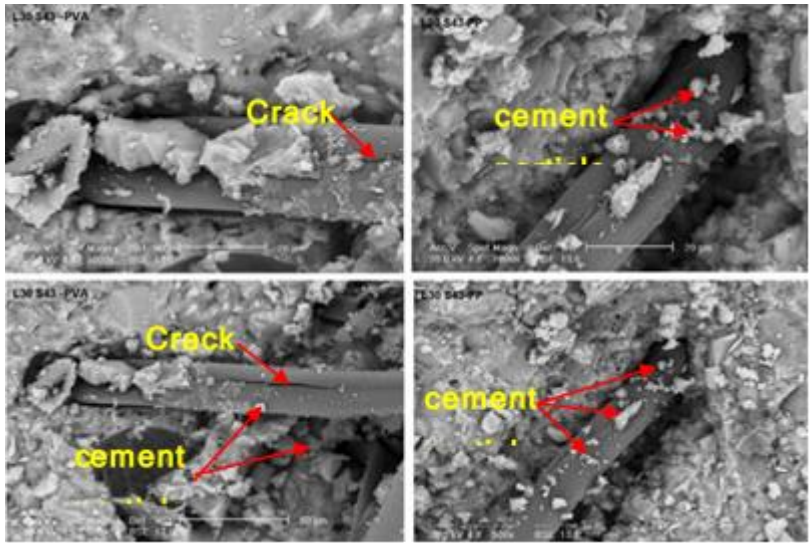

Fig. 13 Post-bending SEM images of 28-day PP-ECC and PVA-ECC specimens

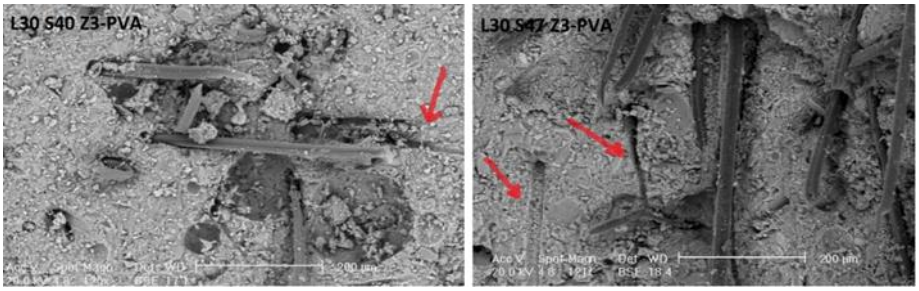

Fig. 14 PVA-ECC fiber pullout path after the bending test

Fig. 14 illustrates the fiber pullout path in L30 S40 Z3-PVA. In fact, after bridging across crack edges, the fibers transfer forces through their development length from one crack edge to the other. The amount of force transferred is a function of both the development length of the fibers and the bond strength at the fiber-matrix interface. The fibers inside the matrix slip if the force applied exceeds fiber capacity. Exploiting this capacity is precisely one of the goals of manufacturing ECCs in this study. Theoretically, on each plane of cracks, the load tolerated by the matrix is taken over by the bridging fibers. The load carried by the bridging fiber is a function of the width opening of the crack and crack opening is a function of fiber bridging characteristics (fiber rupture or fiber slippage). Different combination of fiber-matrix interfacial bond and fiber tensile strength lead to different fiber bridging characteristics, fiber rupture or fiber slippage, and cause differences in the failure mechanism of the ECC [41] . Contrary to intuition, high chemical bond which limits debonding of fiber from matrix is not preferred as it suppresses the fiber slippage as well as multiple cracking creation. Instead, a high frictional bond during fiber slippage is advantageous to maintaining adequate load carrying capacity across the multiple cracks while allowing crack opening to occur in a controlled manner [27] .

4. Conclusion

The mechanical properties and durability of ECC specimens treated in a sulfate medium were experimentally investigated and the effects of silica fume, zeolite, BFS, and fiber type over time were studied on variations in compressive strength, flexural strength, and MSD. Moreover, SEM images were prepared to verify test results. Based on the results obtained, the following conclusions may be drawn:

- Although both PP-ECC and PVA-ECC specimens exhibited multiple cracking patterns and a strain-hardening behavior, the PP-ECC ones showed predominantly higher MSD values and lower compressive and flexural strengths, resulting in their outperformance in a sulfate environment.
- Multiple cracking patterns and crack widths in the PP-ECC specimens were clearly different from those in PVA-ECC ones. The crack width and crack intervals were higher in PP-ECC specimens than those in PVA-ECC ones (PP-ECC crack width was by more than 10 times higher than that of PVA-ECC).
- Compressive and flexural strengths as well as MSD at all concrete ages recorded their highest values in PP-ECC and PVA-ECC specimens containing silica fume and treated under lab conditions. In contrast, the specimens containing silica fume and treated in the sulfate medium were the weakest (i.e., those with the highest reductions in compressive strength, flexural strength, and MSD). This is evidenced by reductions of 37.5%, 34.7%, and 29% in compressive strength, flexural strength, and MSD, respectively, recorded for the 210-day L30 S40 M3-PVA treated in the sulfate medium.

- From among all the mixtures used in both PP-ECC and PVA-ECC specimens, the L30 S47 Z3 one containing the highest BFS content showed the best performance in a sulfate environment at all concrete ages.
- Although an increment of 18% in BFS reduced compression strength in both PP-ECC and PVA-ECC specimens treated under lab conditions, it had different effects on the flexural strength and MSD values of PP-ECC and PVA-ECC specimens under a sulfate medium at all ECC ages such that it led to higher flexural strength and MSD values in the PVA-ECC specimens but to reduced values of the same parameters in the PP-ECC ones.
- Addition of 3% zeolite was observed to enhance the changes in compressive strength, flexural strength, and MSD in both PP-ECC and PVA-ECC specimens treated in a sulfate medium. Moreover, the increased zeolite addition led to the better performance of the ECC in a sulfate environment as evidenced by the average increases of 5.3%, 9.2%, and 14% in the 210-day compressive strength, flexural strength, and MSD, respectively (L30 S40 Z3-PP vs L30 S43-PP).
- SEM imaging showed that the fibers in the PVA-ECC specimens had experienced severe damages while those in the PP-ECC ones experienced only slight scratches; this was attributed to differences in the fiber-matrix bond strengths of PVA-ECC and PP-ECC which led to early and abrupt rupture of PVA fibers and the resulting lower ductility of the PVA-ECC specimens compared to that of PP-ECC ones.

Declaration of Conflicting Interests

The author(s) declared no potential conflicts of interest with respect to the research, authorship, and/or publication of this article.

References

[1] Almohammad-albakkar M, Behfarnia K. Effects of the combined usage of micro and nano-silica on the drying shrinkage and compressive strength of the self-compacting concrete. Journal of Sustainable Cement-Based Materials. 2020:1-19. https://doi.org/10.1080/21650373.2020.1755382

[2] Xing L, Nie G. Analysis on durability of concrete structure of hydropower stations in China. J Hydroelectric Eng. 2003;29(2):27-31.

[3] Charlwood R. Predicting the long term behaviour and service life of concrete dams: na; 2009.

[4] Almohammad-albakkar M, Behfarnia K. Effects of micro and nano-silica on the fresh and hardened properties of self-consolidating concrete.

[5] Nawy E. Control of cracking in concrete structures. Am Concrete Inst Journal & Proceedings. 1972;69(12). https://doi.org/10.14359/11280

[6] Li K, Ma M, Wang X. Experimental study of water flow behaviour in narrow fractures of cementitious materials. Cement and Concrete Composites. 2011;33(10):1009-13. https://doi.org/10.1016/j.cemconcomp.2011.08.005

[7] Han T-S, Feenstra PH, Billington SL. Simulation of highly ductile fiber-reinforced cement-based composite components under cyclic loading. Structural Journal. 2003;100(6):749-57. https://doi.org/10.14359/12841

[8] Tsukamoto M. Tightness of fiber concrete, Darmstadt concrete. Annual Journal on Concrete and Concrete Structures. 1990;5:215-25.

[9] Li VC, Stang H. Elevating FRC material ductility to infrastructure durability. 2004.

[10] Almohammad-albakkar M, Behfarnia K, Mousavi H. Estimation of drying shrinkage in self-compacting concrete containing micro- and nano-silica using appropriate models. Innovative Infrastructure Solutions. 2022;7(5):324. https://doi.org/10.1007/s41062-022-00914-9

[11] Almohammad-albakkar M, Behfarnia K. Water penetration resistance of the self-compacting concrete by the combined addition of micro and nano-silica. Asian Journal of Civil Engineering. 2021;22(1):1-12. https://doi.org/10.1007/s42107-020-00293-5
[12] Li VC. On engineered cementitious composites (ECC). Journal of advanced concrete technology. 2003;1(3):215-30. https://doi.org/10.3151/jact.1.215
[13] Şahmaran M, Li VC. Durability properties of micro-cracked ECC containing high volumes fly ash. Cement and Concrete Research. 2009;39(11):1033-43. https://doi.org/10.1016/j.cemconres.2009.07.009
[14] Wang K, Jansen DC, Shah SP, Karr AF. Permeability study of cracked concrete. Cement and concrete research. 1997;27(3):381-93. https://doi.org/10.1016/S0008-8846(97)00031-8
[15] Aldea CM, Ghandehari M, Shah SP, Karr A. Estimation of water flow through cracked concrete under load. ACI Structural Journal. 2000;97(5):567-75. https://doi.org/10.14359/9289
[16] Aldea C-M, Shah SP, Karr A. Effect of cracking on water and chloride permeability of concrete. Journal of materials in civil engineering. 1999;11(3):181-7. https://doi.org/10.1061/(ASCE)0899-1561(1999)11:3(181)
[17] Aldea C-M, Shah SP, Karr A. Permeability of cracked concrete. Materials and structures. 1999;32(5):370-6. https://doi.org/10.1007/BF02479629
[18] Zhu Y, Zhang H, Zhang Z, Dong B, Liao J. Monitoring the cracking behavior of engineered cementitious composites (ECC) and plain mortar by electrochemical impedance measurement. Construction and Building Materials. 2019;209:195-201. https://doi.org/10.1016/j.conbuildmat.2019.03.132
[19] Banthia N, Sheng J. Fracture toughness of micro-fiber reinforced cement composites. Cement and Concrete Composites. 1996;18(4):251-69. https://doi.org/10.1016/0958-9465(95)00030-5
[20] Lim YM, Li VC. Durable repair of aged infrastructures using trapping mechanism of engineered cementitious composites. Cement and Concrete Composites. 1997;19(4):373-85. https://doi.org/10.1016/S0958-9465(97)00026-7
[21] Maalej M, Quek S, Ahmed S, Zhang J, Lin V, Leong K. Review of potential structural applications of hybrid fiber Engineered Cementitious Composites. Construction and Building Materials. 2012;36:216-27. https://doi.org/10.1016/j.conbuildmat.2012.04.010
[22] Qudah S, Maalej M. Application of Engineered Cementitious Composites (ECC) in interior beam-column connections for enhanced seismic resistance. Engineering Structures. 2014;69:235-45. https://doi.org/10.1016/j.engstruct.2014.03.026
[23] Pan Z, Wu C, Liu J, Wang W, Liu J. Study on mechanical properties of cost-effective polyvinyl alcohol engineered cementitious composites (PVA-ECC). Construction and Building Materials. 2015;78:397-404. https://doi.org/10.1016/j.conbuildmat.2014.12.071
[24] Şahmaran M, Al-Emam M, Yıldırım G, Şimşek YE, Erdem TK, Lachemi M. High-early-strength ductile cementitious composites with characteristics of low early-age shrinkage for repair of infrastructures. Materials and Structures. 2015;48(5):1389-403. https://doi.org/10.1617/s11527-013-0241-z
[25] Meng D, Lee C, Zhang Y. Flexural and shear behaviours of plain and reinforced polyvinyl alcohol-engineered cementitious composite beams. Engineering Structures. 2017;151:261-72. https://doi.org/10.1016/j.engstruct.2017.08.036
[26] Wu C, Li VC. CFRP-ECC hybrid for strengthening of the concrete structures. Composite Structures. 2017;178:372-82. https://doi.org/10.1016/j.compstruct.2017.07.034
[27] Zhang Z, Zhang Q. Matrix tailoring of engineered cementitious composites (ECC) with non-oil-coated, low tensile strength PVA fiber. Construction and Building Materials. 2018;161:420-31. https://doi.org/10.1016/j.conbuildmat.2017.11.072

[28] Arulanandam PM, Sivasubramnaian MV, Chellapandian M, Murali G, Vatin NI. Analytical and Numerical Investigation of the Behavior of Engineered Cementitious Composite Members under Shear Loads. Materials. 2022;15(13):4640. https://doi.org/10.3390/ma15134640
[29] Maheswaran J, Chellapandian M, Sivasubramanian MV, Murali G, Vatin NI. Experimental and Numerical Investigation on the Shear Behavior of Engineered Cementitious Composite Beams with Hybrid Fibers. Materials. 2022;15(14):5059. https://doi.org/10.3390/ma15145059
[30] Lepech M, Li VC, editors. Durability and long term performance of engineered cementitious composites. Proceedings of the International Workshop on HPFRCC in Structural Applications; 2005.
[31] Gao S, Zhao X, Qiao J, Guo Y, Hu G. Study on the bonding properties of Engineered Cementitious Composites (ECC) and existing concrete exposed to high temperature. Construction and Building Materials. 2019;196:330-44. https://doi.org/10.1016/j.conbuildmat.2018.11.136
[32] Kan L-l, Shi R-x, Zhu J. Effect of fineness and calcium content of fly ash on the mechanical properties of Engineered Cementitious Composites (ECC). Construction and Building Materials. 2019;209:476-84. https://doi.org/10.1016/j.conbuildmat.2019.03.129
[33] Wu H-L, Yu J, Zhang D, Zheng J-X, Li VC. Effect of morphological parameters of natural sand on mechanical properties of engineered cementitious composites. Cement and Concrete Composites. 2019;100:108-19. https://doi.org/10.1016/j.cemconcomp.2019.04.007
[34] Jiang L, Niu D. Study of deterioration of concrete exposed to different types of sulfate solutions under drying-wetting cycles. Construction and Building Materials. 2016;117:88-98. https://doi.org/10.1016/j.conbuildmat.2016.04.094
[35] Hashemi S. Experimental study on mechanical properties of different lightweight aggregate concretes. Engineering Solid Mechanics. 2014;2(3):201-8. https://doi.org/10.5267/j.esm.2014.4.003
[36] Behfarnia K, Farshadfar O. The effects of pozzolanic binders and polypropylene fibers on durability of SCC to magnesium sulfate attack. Construction and Building Materials. 2013;38:64-71. https://doi.org/10.1016/j.conbuildmat.2012.08.035
[37] Hekal EE, Kishar E, Mostafa H. Magnesium sulfate attack on hardened blended cement pastes under different circumstances. Cement and Concrete Research. 2002;32(9):1421-7. https://doi.org/10.1016/S0008-8846(02)00801-3
[38] Al-Amoudi OSB. Attack on plain and blended cements exposed to aggressive sulfate environments. Cement and Concrete Composites. 2002;24(3-4):305-16. https://doi.org/10.1016/S0958-9465(01)00082-8
[39] Park Y-S, Suh J-K, Lee J-H, Shin Y-S. Strength deterioration of high strength concrete in sulfate environment. Cement and concrete research. 1999;29(9):1397-402. https://doi.org/10.1016/S0008-8846(99)00106-4
[40] Ananthi A, Karthikeyan J. Combined Performance of Polypropylene Fibre and Weld Slag in High Performance Concrete. Journal of The Institution of Engineers (India): Series A. 2017;98(4):405-12. https://doi.org/10.1007/s40030-017-0248-5
[41] Suthiwarapirak P, Matsumoto T, Kanda T. Multiple cracking and fiber bridging characteristics of engineered cementitious composites under fatigue flexure. Journal of materials in civil engineering. 2004;16(5):433-43. https://doi.org/10.1061/(ASCE)0899-1561(2004)16:5(433)